Determining topographical radiation dose profiles using gel nanosensors

November 25 2019, by Thamarasee Jeewandara

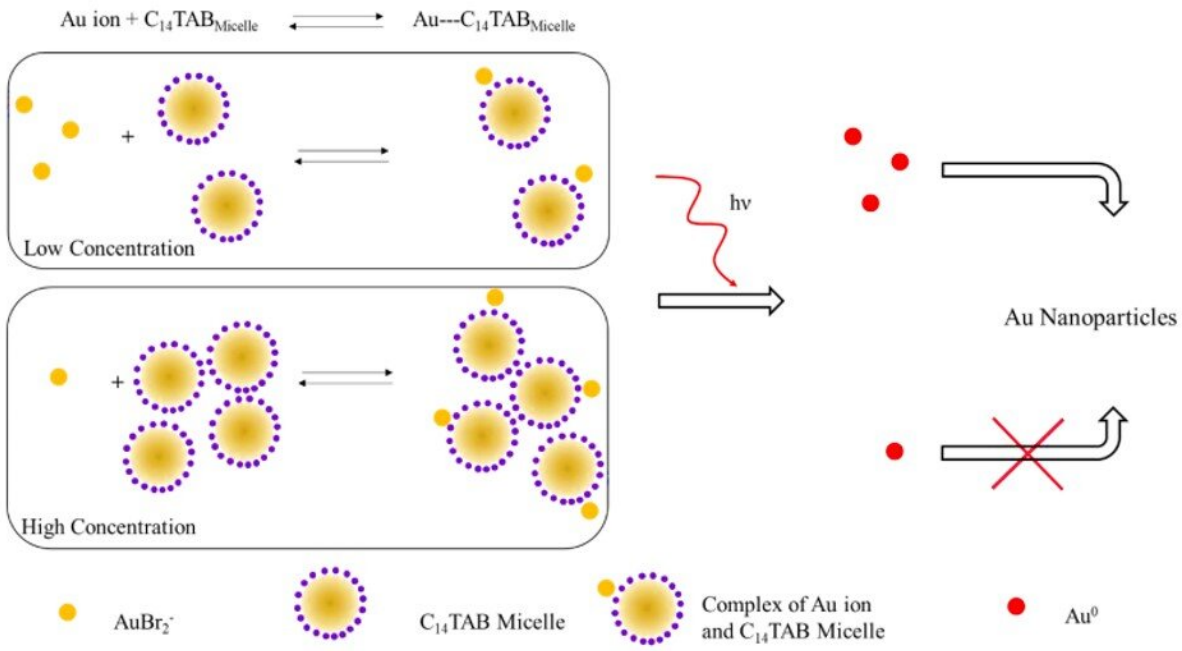

Schematic illustration of the proposed mechanism for the formation of gold nanoparticles upon irradiation with ionizing radiation. At low surfactant concentrations, most gold ions (AuBr2- /Au1+) are likely free in solution (unbound to micelles). With increasing surfactant concentration, the equilibrium shifts to the right with a decrease in free gold ions. Upon irradiation, the number of Au^0 atoms formed due to reduction at low surfactant concentration is higher due to the presence of a higher number of free gold ions in contrast to the system at high surfactant concentration. The higher number of free gold atoms leads to an increased yield of gold nanoparticles due to surface-assisted reduction with unreacted gold ions. Credit: Science Advances, doi: 10.1126/sciadv.aaw8704.

The routine measurement of radiation doses can be clinically challenging due to limitations with conventional dosimeters used to measure the dose uptake of external ionizing radiation. In a new study, Karthik Pushpavanam and an interdisciplinary team of researchers in the departments of Chemical Engineering, Molecular Sciences, Banner MD Anderson Cancer Center and Arizona Veterinary Oncology in the U.S. has described a novel gel-based nanosensor. The technology allows colorimetric detection and quantification of topographical radiation dose profiles during radiotherapy.

Upon exposure to ionizing radiation, the scientists converted gold ions in the gel in to gold nanoparticles (AuNPs) accompanied with a visual change in gel color due to plasmonic properties. They used the intensity of color formed in the gel as a quantitative reporter for ionizing radiation and first used the gel nanosensor to detect complex topographical dose patterns after administration to anthropomorphic phantom models followed by applications with live canine patients undergoing clinical radiotherapy. The ease of fabrication, operation, rapid readout, colorimetric detection and relatively low cost of the technology implied translational potential for topographical dose mapping during clinical radiotherapy applications. The research work is now published on *Science Advances*.

Advances in radiation therapy have led to notable sophistication and state-of-the-art planning software to deliver high conformal radiation doses to patients for improved quality of life after treatment. During radiotherapy, a high dose is typically delivered to a target tumor while minimizing the radiation dose delivered to surrounding tissue. During palliative care patients are administered with larger fractional doses in order to conclude treatment within a short time frame. However, software errors during such procedures can lead to overdosing and subsequent morbidity.

To minimize accidental overexposure, researchers seek to independently verify the dose of radiation delivered at or near the target tissue for advanced patient safety. Technically, both molecular and nanosensors can overcome limits present in conventional systems to form practical alternatives as facile sensors. However, their existing limits should be addressed and alleviated to develop robust and effective sensors that quantitatively and qualitatively determine the topographical dose profiles during clinical radiotherapy.

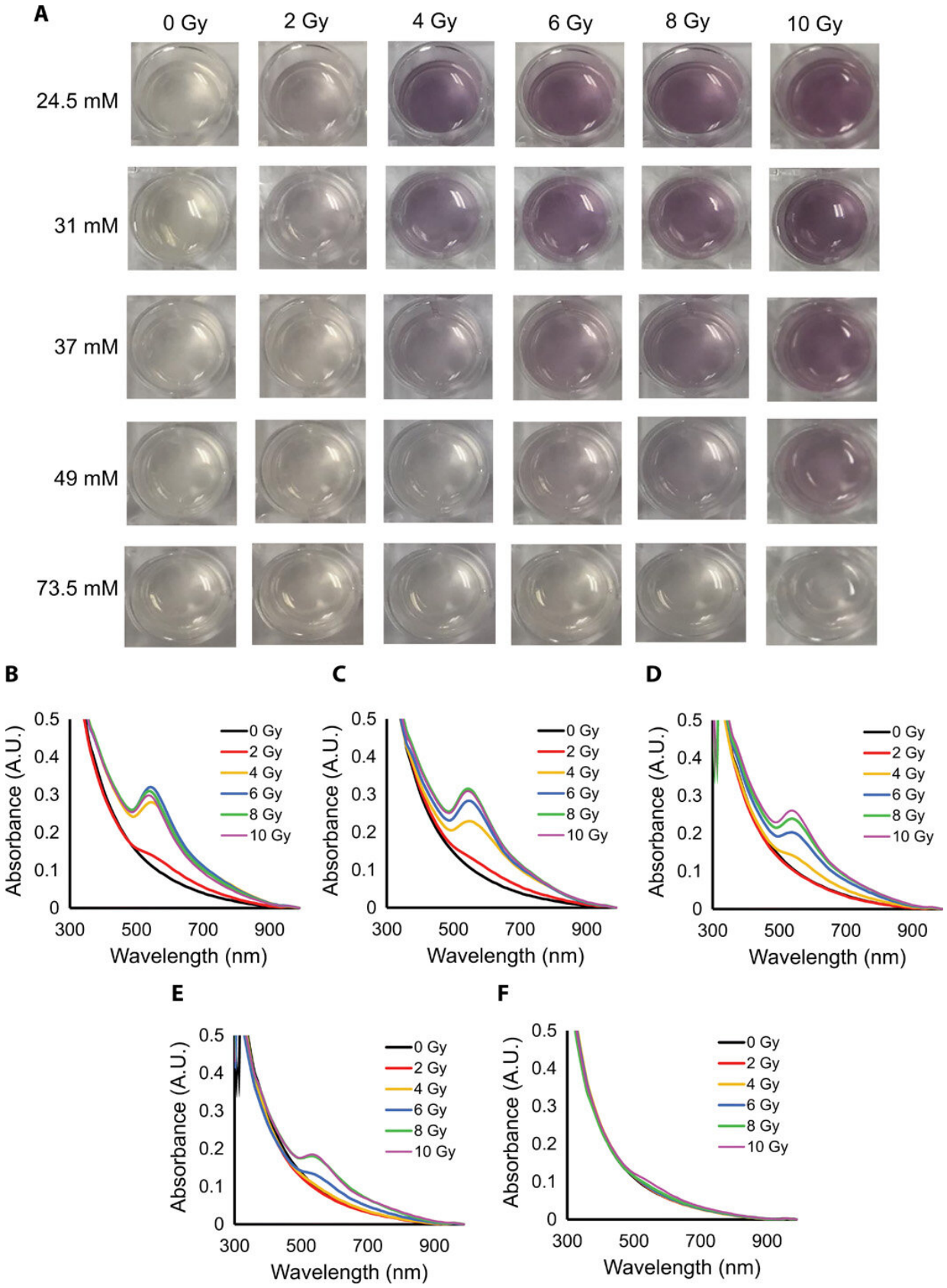
A
0 Gy
2 Gy
4 Gy
6 Gy
8 Gy
10 Gy
24.5 mM
31 mM
37 mM
49 mM
73.5 mM
B
C
D
E
F
Absorbance (A.U.)
Wavelength (nm)
0 Gy
2 Gy
4 Gy
6 Gy
8 Gy
10 Gy

Digital images and UV-visible spectra of different gel nanosensor formulations exposed to therapeutic doses of x-rays (A) Images of gel nanosensors fabricated in 24-well cell culture plates and containing different concentrations of C14TAB (24.5 to 73.5 mM) upon exposure to various doses of ionizing radiation (0- to 10-Gy x-rays); Na2S wait time was 5 min after irradiation, and incubation time was 10 min. Images were acquired 1 hour after irradiation. A visible increase in intensity in the maroon color is observed with increasing doses of ionizing radiation for most C14TAB concentrations used during gel sensor development. (B to F) Absorbance spectra (300 to 990 nm) of the same gel nanosensors containing (B) 24.5 mM, (C) 31 mM, (D) 37 mM, (E) 49 mM, and (F) 73.5 mM irradiated using different radiation doses. Characteristic absorbance peaks between 500- and 600-nm wavelengths are indicative of gold nanoparticles formed in the gels. The corresponding radiation doses are mentioned in the legend with increasing radiation dose (top to bottom). A.U., arbitrary units. Photo credit: Sahil Inamdar, Arizona State University. Credit: Science Advances, doi: 10.1126/sciadv.aaw8704

Since gold nanoparticles (AuNPs) have unique physical and chemical characteristics that provide an excellent platform to develop sensors. Pushpavanam et al. engineered a colorimetric sensor where ionizing radiation caused AuNP formation from colorless salt precursors. The formation of a gel-based nanosensor can allow easy handling and applications during clinical radiotherapy.

In the present work, the team demonstrated colorimetric detection and quantification of dose distribution profiles using a gel nanosensor to topographically map radiation doses along tissue surfaces. During preclinical evaluations, the team administered the gel nanosensor technology in live canine patients undergoing radiotherapy. In total, the results indicated the scope of the technology for clinical translation in human patients and the capacity to determine topographic doses to plan

treatments and verify dosages during cancer radiotherapy.

During the experiments, the conversion of gold ions into nanoparticles was accompanied by a maroon color development in the irradiated region of the gel nanosensor. While gold exists in a trivalent state in general ($AuCl_4^-$) it can be reduced to a metastable +1 valence state ($AuBr_2^-$) at room temperature using ascorbic acid (Vitamin C). The irradiation of gels containing therapeutic levels of radiation stimulated radiolysis or the splitting of water molecules into highly reactive free radicals. The radiolysis-generated hydrated electrons in turn reduced monovalent gold to form gold atoms in its zerovalent state (Au^0) that nucleated and matured into maroon colored AuNPs. The intensity varied with the dose of radiation and the team used the range of linear responses to calibrate the gel nanosensor. Based on this principle, Pushpavanam et al. determined the response of the fully irradiated gels to calibrate absorbance with radiation dose.

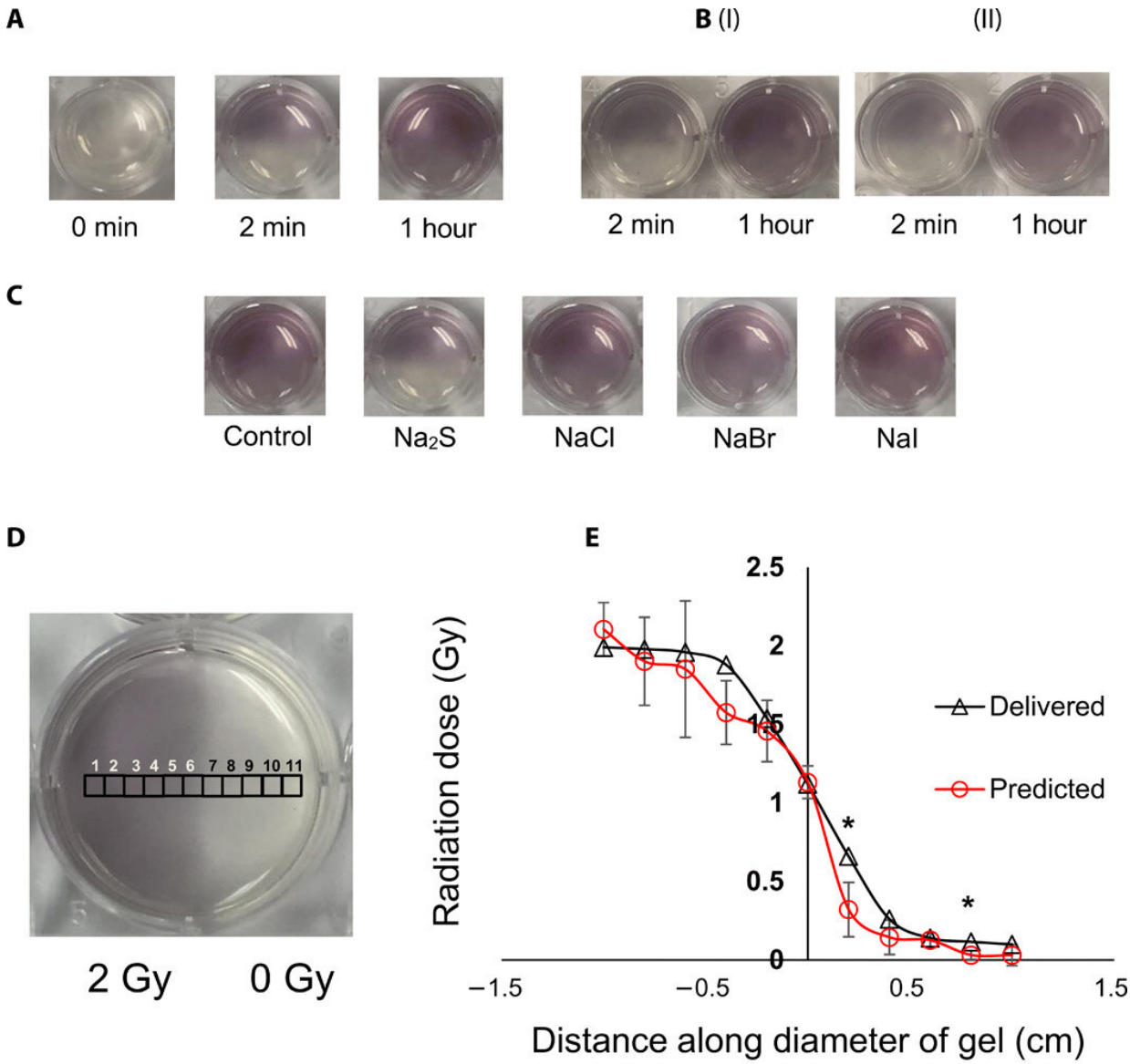

Topographical visualization and quantification of radiation doses using gel

nanosensors. (A) Gel nanosensor (left) before irradiation, (middle) top half irradiated with 4 Gy and image acquired 2 min after irradiation, and (right) image acquired 1 hour after irradiation. A visible increase in color intensity in the nonirradiated lower half indicates bleed over of color and loss of topographical information. (B) I: 1.5% (w/v) agarose gel (left) 2 min after irradiation and (right) 1 hour after irradiation; II: 2% (w/v) agarose gel (left) 2 min after irradiation and (right) 1 hour after irradiation indicates that the increase in agarose weight percentage does not preserve topographical dose information. (C) Gel nanosensor incubated with 5 mM sodium sulfide (Na2S) and various sodium halides with a wait time of 10 min and incubation time of 10 min; images were acquired after 1 hour. No loss of topographical information is observed upon incubation with sodium sulfide. All gels were fabricated in 24-well plates. (D) Colorimetric response of the gel nanosenor irradiated on one-half with a 2-Gy x-ray dose. A visible appearance of maroon color in the irradiated region illustrates the ability of the gel nanosensor to visualize topographical dose profiles. Each black square box (labeled 1 to 11) on the gel nanosensor corresponds to a grid of size ≈2 × 2 mm, whose absorbance at 540 nm is determined. Grids starting from 1 to 5 are regions exposed to ionizing radiation, 6 is the grid at the edge of the irradiation field, and grids from 7 to 11 are regions outside the field of irradiation. (E) Dose fall-off profile for the gel nanosensor irradiated by 2 Gy on one-half. The delivered and predicted radiation doses are comparable, which indicates the efficacy of the gel nanosensor in visualizing and retaining topographical information. In all cases, Na2S was added for 10-min incubation time after a wait time of 30 min. Radiation doses predicted by the gel nanosensor as compared with the delivered radiation dose as obtained from the treatment planning system. Asterisks indicate statistically significant differences (P

To determine intensity of the color and dose delivered within gels after irradiation, the researchers used absorbance spectroscopy and observed a decrease in the spectral profile width, with increasing radiation dose for decreased polydispersity (ratio of the percentage of the standard deviation to the average value) of the nanoparticles. The peak absorbance intensity increased with increasing radiation dose to corroborate the observed increase in color intensity.

To understand the gel nanosensor's ability to detect topographical distribution of the radiation dose, the scientists irradiated half of the gel nanosensor with a 4 gray (Gy) dose. The maroon-color only appeared in the irradiated area confirming AuNP formation, but after one hour of exposure, the color bled into the irradiated region showing loss of topographic information in the gel with time. The team observed the phenomenon to arise from reaction-controlled conditions and not based on the gel composition. By incubating the gel with sodium sulfide (Na_2S) for 10 minutes, they suppressed the color bleed-over and reasoned that to the ability to quench unreacted gold ions in the nonirradiated region and preserve dose information accurately for dose visualization and dosimetry. The scientists adopted the sensor for wide dose ranges by modulating the time of Na_2S addition; to achieve a level of flexibility hitherto unavailable in clinical dose detection systems.

The research team then used the gel nanosensor to visualize diverse topographical radiation patterns, where the intensity of the color increased with increasing dose while preserving topographical integrity. As proof of concept, they showed the gel nanosensor's ability to detect complex radiation patterns with a model dose patterned to form "ASU" (after Arizona State University). Then using transmission electron microscopy (TEM), the scientists characterized the generated gold nanoparticles as a function of dose to observe reduced average nanoparticle diameter and polydispersity at higher doses of radiation. They followed this with energy dispersive X-ray spectroscopy (EDS) to detect higher yields of AuNPs in the irradiated regions of the gel nanosensor as expected.

A

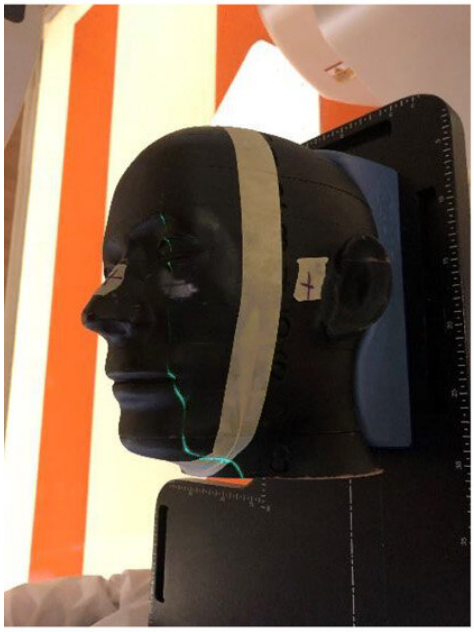

B

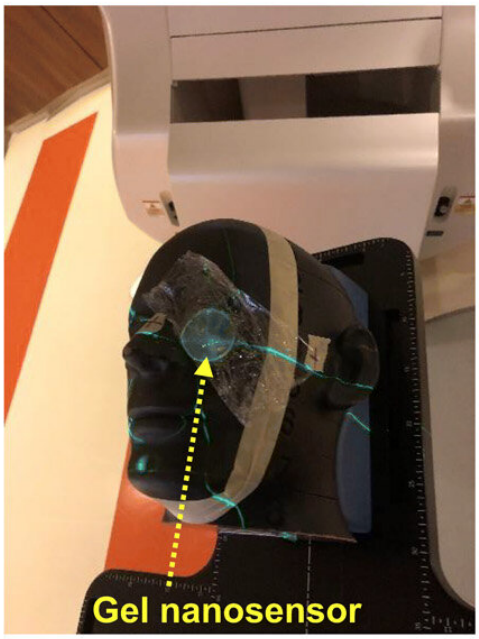

C

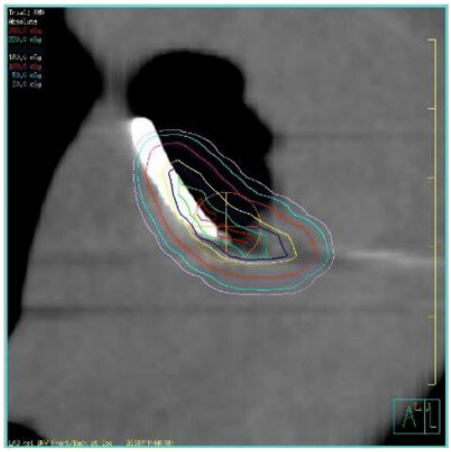

D

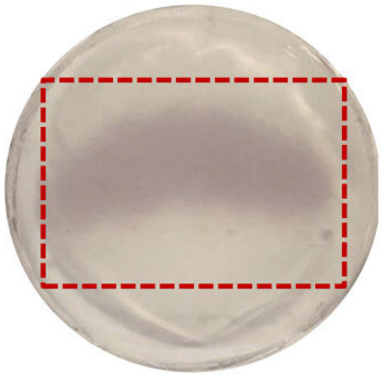

E

	0.0	0.0	0.0	0.0	0.0	0.1	0.0	0.0	0.0	
0.0	0.0	0.1	0.1	0.2	0.2	0.2	0.1	0.1	0.0	0.0
0.1	0.1	0.3	0.7	0.8	0.9	0.7	0.5	0.2	0.1	0.0
0.2	0.6	1.1	1.6	1.9	1.9	1.8	1.4	0.8	0.4	0.1
0.4	1.2	2.0	2.2	2.3	2.3	2.3	2.2	1.7	1.0	0.3
0.7	1.4	1.9	2.0	2.0	2.0	2.1	2.2	2.1	1.6	0.7
0.3	0.8	0.9	1.0	0.9	0.8	1.1	1.4	1.5	1.4	0.6
0.1	0.2	0.2	0.2	0.2	0.2	0.3	0.4	0.5	0.4	0.2
0.0	0.0	0.1	0.1	0.1	0.1	0.1	0.1	0.1	0.1	0.1
	0.0	0.0	0.0	0.0	0.0	0.0	0.0	0.0	0.0	

F

	0.2	0.0	0.0	0.0	0.0	0.0	0.0	0.1	0.4	
0.3	0.0	0.0	0.4	0.0	0.4	0.1	0.1	0.0	0.0	0.1
0.0	0.4	1.6	1.7	2.0	2.1	1.9	1.8	0.7	0.1	0.0
0.2	1.1	1.9	2.2	2.3	2.4	2.4	2.3	2.1	1.6	1.3
2.0	2.3	2.4	2.3	2.3	2.3	2.4	2.5	2.3	2.2	1.8
1.9	2.3	2.1	2.3	1.6	1.3	1.7	1.8	1.9	2.1	1.9
1.2	0.9	0.9	0.3	0.1	0.1	0.2	0.3	0.4	0.5	0.3
0.1	0.0	0.0	0.0	0.0	0.0	0.0	0.0	0.0	0.0	0.0
0.3	0.0	0.0	0.0	0.0	0.0	0.0	0.1	0.0	0.0	0.2
	0.5	0.2	0.1	0.0	0.1	0.1	0.1	0.4	0.4	

Gel nanosensor enabled topographical detection and quantification of clinical radiation doses in anthropomorphic head and neck phantoms. (A) Anthropomorphic head and neck phantom treated with an irregularly shaped x-ray radiation field below the left eye. (B) Image of the gel nanosensor positioned on the anthropomorphic phantom in the radiation field mimicking a conventional radiotherapy session. (C) Axial view of the treatment planning image along the central axis of the radiation beam representing an irregularly shaped radiation field used to deliver a complex radiation pattern under the eye of the phantom. The core of the crescent-shaped treatment region receives a radiation dose of 2.3 Gy (highlighted in red), and regions receiving lower doses are highlighted with different colors going outward (from green to light pink). (D) Visual image of the dose pattern on the gel nanosensor formed after delivery of 2.3 Gy. Only the irradiated region develops a maroon color, while the nonirradiated region remains colorless. (E) Expected topographical dose "heat map" profile of the radiation dose delivered to the gel placed in the phantom. The expected profile is generated from the treatment plan in the dose delivery system. In these figures, red and blue colors indicate higher and lower radiation doses, respectively. (F) Topographical doses predicted by the irradiated gel nanosensor. Absorbance values of ≈2 mm × 2 mm grids were quantified using a calibration curve to generate the topographical dose profile. The anticipated dose received by the core of the crescent-shaped profile (2.3 Gy) is comparable to the dose profile predicted by the gel nanosensor (2.3 Gy), which demonstrates the capability of the gel nanosensor to qualitatively and quantitatively detect complex topographical dose profiles. Photo credit: Sahil Inamdar, Arizona State University. Credit: Science Advances, doi: 10.1126/sciadv.aaw8704.

To investigate translational potential of the gel nanosensor and predict topographical profiles of radiation, Pushpavanam et al. first used a head and neck phantom model. They delivered an irregular crescent-shaped radiation dose near the eye to mimic clinically challenging administration modes of radiotherapy close to critical structures such as the eye during skin cancer treatment. The dose profile delivered using the treatment planning system was in excellent agreement with the predictions of the gel nanosensor. Indicating its capability to detect and predict complex radiation patterns similar to those used in clinical human radiotherapy.

During preclinical studies, the research team used two canine models undergoing

radiotherapy to investigate the efficiency of gel nanosensors as independent, nanoscale radiation dosimeters for the first time and compared the efficiency with conventional clinical radiochromic films. On completion of the treatment, Pushpavanam et al. observed maroon color formation in one-half of the gel, whereas the non-irradiated region remained colorless. They showed predictions of the gel nanosensor in the irradiated region to agree excellently with the treatment planning system and the radiochromic film. The gel nanosensor also predicted for the region external to the irradiation to receive minimal radiation and their topographical dose profiles as well. The performance was comparable to clinical radiochromic films but with faster than conventional wait times (typically >24 hours) to obtain the results. The scientists demonstrated the simplicity of fabrication, operation, readout time and cost effectiveness ($ 0.50 per gel material only) of the frugal invention. They maintained the response of the gel nanosensor for at least seven days to indicate long-term retrieval of dosing data unlike with fluorescence-based dosimeters with readouts that lasts mere minutes.

A

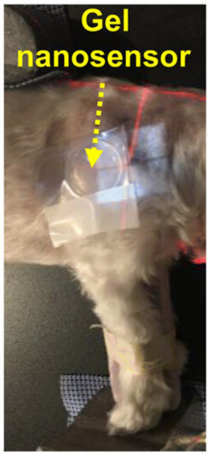

B

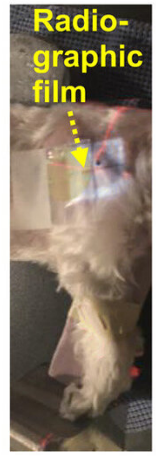

C

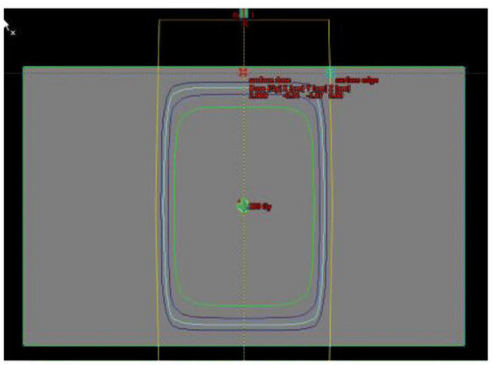

D

2.0	2.0	2.0	2.0	1.6	0.9	0.3	0.1	0.1
2.0	2.0	2.0	2.0	1.6	0.9	0.3	0.1	0.1
2.0	2.0	2.0	2.0	1.6	0.9	0.3	0.1	0.1
2.0	2.0	2.0	2.0	1.6	0.9	0.3	0.1	0.1
2.0	2.0	2.0	2.0	1.6	0.9	0.3	0.1	0.1
2.0	2.0	2.0	2.0	1.6	0.9	0.3	0.1	0.1
2.0	2.0	2.0	2.0	1.6	0.9	0.3	0.1	0.1
2.0	2.0	2.0	2.0	1.6	0.9	0.3	0.1	0.1
2.0	2.0	2.0	2.0	1.6	0.9	0.3	0.1	0.1

E

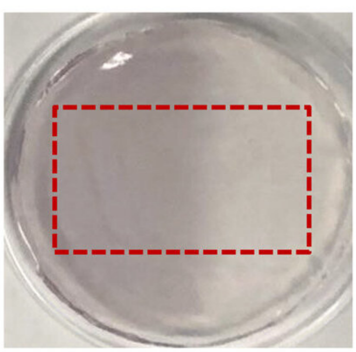

2.4	2.2	2.2	1.9	1.1	0.1	0.0	0.1	0.1
2.2	2.1	2.0	1.7	0.6	0.0	0.0	0.1	0.1
2.1	2.0	2.0	1.8	1.0	0.2	0.0	0.0	0.1
2.1	2.0	2.0	1.7	0.7	0.2	0.1	0.0	0.1
2.2	2.0	2.0	1.9	1.1	0.1	0.0	0.1	0.1
2.0	2.0	2.0	1.9	0.8	0.0	0.0	0.1	0.1
2.1	2.0	2.0	1.9	1.3	0.1	0.1	0.1	0.2
2.3	2.1	2.1	2.0	1.0	0.1	0.1	0.1	0.1
2.4	2.4	2.4	2.1	1.2	0.4	0.2	0.1	0.3

F

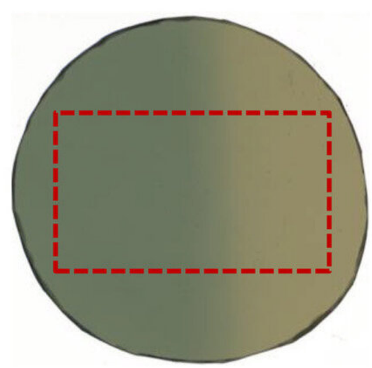

2.2	2.2	2.3	2.1	1.5	0.5	0.2	0.1	0.0
2.2	2.2	2.2	2.1	1.5	0.5	0.1	0.1	0.0
2.2	2.2	2.2	2.1	1.5	0.5	0.1	0.0	0.0
2.2	2.1	2.1	2.1	1.5	0.5	0.1	0.1	0.0
2.2	2.1	2.2	2.1	1.6	0.5	0.1	0.0	0.0
2.2	2.2	2.1	2.0	1.5	0.5	0.1	0.0	0.0
2.1	2.2	2.1	2.0	1.5	0.6	0.2	0.0	0.0
2.0	2.2	2.1	2.1	1.6	0.7	0.1	0.0	0.0
2.0	2.1	2.1	2.0	1.6	0.7	0.1	0.0	0.0

Gel nanosensor enabled topographical detection and quantification of radiation delivered to canine patient A undergoing clinical radiotherapy. Representative image of (A) half of the gel nanosensor and (B) half of the radiographic film positioned in the radiation field delivered to canine patient A. (C) Treatment planning software depicting the delivery of a 2-Gy dose delivered to the surface of patient A (neon green edge along the rectangular gray box indicates the region receiving the 2-Gy dose). (D) The irradiated region received a dose of 2 Gy (highlighted in red squares), with irradiation dose dropping to a minimal radiation 0.1 Gy (highlighted in blue squares) outside the field of irradiation. A color change is visible in both the (E) gel nanosensor whose color changes to maroon and (F) radiographic film whose color changes to dark green after irradiation. The predicted dose map in the gel nanosensor (Na2S addition wait time of 30 min and incubation time of 10 min) and radiographic film are shown below each corresponding sensor. Similarity in the dose profiles indicates the efficacy of the gel nanosensor for clinical dosimetry. The time for readout of the gel nanosensor was 1 hour after irradiation, while the radiochromic film required >24 hours of developing time before readout. All experiments were carried out three independent times. Photo credit: Sahil Inamdar, Arizona State University. Credit: Science Advances, doi: 10.1126/sciadv.aaw8704.

In this way, Karthik Pushpavanam and colleagues developed the first colorimetric gel nanosensor as a nanoscale dosimeter to detect and distinguish regions exposed to irradiation. They optimized the platform with a chemical quenching agent (Na_2S) to accurately reveal topographical dose distribution during clinical radiotherapy. The scientists can control the pore size distribution of the gel substrate to enhance efficacy of the nanosensor. They tested the efficiency of the gel nanosensor to predict complex topographical dose profiles in anthromorphic head and neck phantoms and in live canine patients undergoing radiotherapy. The highly disruptive and translational potential of the gel nanosensor technology will lead to improved patient safety and outcomes in clinical radiotherapy.

More information: Karthik Pushpavanam et al. Determination of topographical radiation dose profiles using gel nanosensors, *Science Advances* (2019). DOI: 10.1126/sciadv.aaw8704

Karthik Pushpavanam et al. A Colorimetric Plasmonic Nanosensor for Dosimetry of Therapeutic Levels of Ionizing Radiation, *ACS Nano* (2015). DOI: 10.1021/acsnano.5b05113

Nashrulhaq Tagiling et al. Effect of scanning parameters on dose-response of radiochromic films irradiated with photon and electron beams, *Heliyon* (2018). DOI: 10.1016/j.heliyon.2018.e00864